Model Updating with Experimental Frequency Response Function Considering General Damping

Yu Hong[1,2], Qianhui Pu*[1], Yang Wang[2], Liangjun Chen[1], Hongye Gou[1], Xiaobin Li[1]

1. School of Civil Engineering, Southwest Jiaotong University, Chengdu, 610031, China;

2. School of Civil and Environmental Engineering, Georgia Institute of Technology, Atlanta, 30332, USA

Abstract: In order to obtain a more accurate finite element (FE) model of a constructed structure, a new frequency response function (FRF)-based model updating approach is proposed. A general viscous damping model is assumed in this approach for better simulating the actual structure. The approach is formulated as an optimization problem which intends to minimize the difference between analytical and experimental FRFs. Neither dynamic expansion nor model reduction is needed when not all degrees of freedom are measured. State-of-the-art optimization algorithms are utilized for solving the non-convex optimization problem. The effectiveness of the presented FRF model updating approach is validated through a laboratory experiment on a four-story shear-frame structure. To obtain the experimental FRFs, a shake table test was conducted. The proposed FRF model updating approach is shown to successfully update the stiffness, mass and damping parameters in matching the analytical FRFs with the experimental FRFs. In addition, the updating results are also verified by comparing time-domain experimental responses with the simulated responses from the updated model.

Keywords: frequency response function; finite element model updating; general viscous damping; non-convex optimization; shake table test

1 Introduction

With rapid development in numerical simulations, FE analysis has become a more and more powerful tool in structural engineering. Although significant improvements have been made towards accurate FE modeling, in general, there are still distinct differences between behaviors of a constructed structure and these of the FE model built according to the same design drawings. It is well known that

[1] **Corresponding author**: Qianhui Pu, Professor; Tel: +86-13908003012; E-mail:qhpu@vip.163.com

analytical results from FE model often differ from performance of an actual structure in the field. The mismatch is mainly caused by nominal material property values, idealized boundary conditions, difficulties in modeling of damping, etc. To achieve an FE model that more accurately represents the actual structure, FE model updating can be performed through calibration with high-fidelity experimental test data. An accurate FE model can also be used later for structural safety monitoring and damage detection.

A number of FE model updating approaches have been proposed and practically applied during the past few decades, as reviewed by Imregun and Visser (1991). Friswell and Mottershead (1995) discussed detailed model updating techniques in their book. Most model updating approaches can be broadly categorized into time domain approaches and frequency domain approaches. Time domain approaches usually use vibration data to directly update the FE model (Yang *et al*. 2009; Hernandez and Bernal 2013). Although they have merits, the computational efforts are usually a concern. On the other hand, in frequency domain, most approaches need to use the experimental modal properties of a structure to construct an optimization problem for model updating (Zhu *et al*. 2016; Brito *et al*. 2014; Jaishi and Ren 2005; Tshilidzi and Sibusiso 2005). The optimization problem generally attempts to minimize an objective function that contains the difference between experimental and simulated natural frequencies, mode shapes and modal flexibilities, etc. In these model updating approaches, extraction of modal properties from experimental data is first required, which can add uncertainties and inaccuracies to the updating. In addition, in most cases, only limited amount of modal information can be obtained from modal analysis. As summarized by Jaishi and Ren (2005), an accurate model can be achieved only when the number of extracted experimental modal properties is greater than or equal to the number of interested updating variables.

This research focuses on another category in frequency domain model updating approaches, which is based on frequency response functions (FRF). From experimental data, FRFs can be easily calculated using excitation record and corresponding structural responses. This avoids the need for extracting modal properties and the associated extraction errors. Furthermore, high quality FRFs can be obtained by using FRF estimators to minimize the influence of noise in the calculation (Schoukens and Pintelon

1990; Antoni *et al*. 2004). Another advantage of FRF-based approaches is that an experimental test can provide abundant FRF data in a large frequency range. Owing to these advantages, FRF-based approaches constitute a highly valuable category in FE model updating.

Among the most widely known FRF-based model updating approaches was proposed by Lin and Ewins (1994), which avoids the inverse of the system dynamic stiffness matrix by using the analytical FRF sensitivity matrix. This approach usually can perform accurately and efficiently on numerical simulation cases, because of the assumptions of noise-free and complete measurements on all degrees of freedoms (DOFs). However, such assumptions, particularly the sensor instrumentation on all DOFs, are usually unrealistic in practice. Through model reduction technique, Asma and Bouazzouni (2005) later extended Lin and Ewins' work to update a truss structure with incomplete measurement. Alternatively, Avitabile and O'callaham (2001) presented the dynamic expansion approach to get a full column or row of an FRF matrix. Nevertheless, it is well known that neither reduction nor expansion can fully describe the actual dynamic behavior of a structure. To overcome this limitation, Sipple and Sanayei (2014) proposed a numerically evaluated FRF sensitivity-based model updating approach. Optimization techniques are utilized to iteratively change the analytical FRFs to match the experimental counterparts. The modal-decomposed analytical FRF is in scalar form which can be directly used in updating process. The model reduction or dynamic expansion is not necessary in this case.

Due to the existence of damping, the experimental FRFs are usually complex valued functions. Despite the large amount of literature on damping modeling, damping still remains the least known aspect compared with stiffness and mass. In order to avoid the difficulties in damping updating, Pradhan and Modak (2012) proposed to use the real-valued normal FRF matrix $(-\omega^2\boldsymbol{M}+\boldsymbol{K})$ in model updating. However, when formulating the estimation of the normal FRFs, the method requires the full complex-valued FRF matrix which has to be estimated through the identified modal properties. The estimation may still require modal identification and add inaccuracies. Since damping cannot be ignored in practical modeling, especially with complex FRFs, a proper selection of damping model may improve the model updating accuracy. Among all damping models, viscous damping is the most commonly used due to its convenience in structural design. Another model, hysteretic damping, can more accurately describe the energy dissipation in structure vibration, the difficulty of translating this damping mechanism into time domain prevents an easy adoption. In addition, Lim and Zhu (2009) demonstrated that the difference caused by arbitrarily choosing hysteretic damping and viscous damping in system identification is small. Therefore, most researchers prefer to assume proportional viscous damping (i.e. Rayleigh damping or Caughey damping) for FRF-based model updating. For example, Imregun *et al*. (1995) and Hong *et al*. (2016) updated the Rayleigh damping coefficients through an extended FRF-based model updating approach. Lu and Tu (2004), Sipple and Sanayei (2014) updated the damping ratios (corresponding to Caughey damping) in their FRF-based model updating. Nevertheless, proportional damping may rarely exist in reality, and most structures possess non-proportional damping. From this point of view, the use of proportional damping will more or less affect the updating accuracy. A general viscous damping model (which includes both proportional damping and non-proportional damping) can render more accurate model updating.

This research departs from the authors' preliminary study (Hong *et al*. 2016). We focus on a model updating approach that can minimize the difference between analytical and experimental FRFs directly at measured DOFs. This differs from most FRF-based model updating approaches in literature that need reduction or expansion techniques. In comparison with Sipple and Sanayei (2014) and Hong *et al*. (2016), a general viscous damping assumption is provided for better simulating actual structures in reality. The FRF formulation is derived for a base excitation setup when ground vibration occurs to a shear-frame building structure (which effectively applies excitation simultaneously at all DOFs). To validate the proposed FRF-based model updating, shake table tests are performed on a four-story laboratory structure in this study, although the authors are currently extending the formulation for future application to a space frame bridge. The rest of the paper is organized as follows. First, Section 2 presents the analytical FRF formulation for a structure undergoing ground excitation and the experimental FRF calculation. In section 3, the vector form of the analytical FRF to be used in model updating is introduced; then the optimization procedure is discussed. Section 4 describes the shake table test on a four-story aluminum structure for validating the performance of the proposed formulations for FRF-based model updating. We compare the experimentally measured frequency domain FRFs and time domain response histories with their counterparts simulated using the updated model. Finally, conclusions and future work are provided in Section 5.

2 Formulations of the frequency response functions

2.1 Analytical formulation of the frequency response functions considering general viscous damping

Consider the dynamic equation of motion of an *n*-DOF structure with viscous damping at time *t*:

$$\boldsymbol{M}\ddot{\boldsymbol{q}}(t) + \boldsymbol{C}\dot{\boldsymbol{q}}(t) + \boldsymbol{K}\boldsymbol{q}(t) = \boldsymbol{F}(t) \tag{1}$$

where $\boldsymbol{M}, \boldsymbol{K}, \boldsymbol{C} \in \mathbb{R}^{n\times n}$ are mass, stiffness and damping matrices, respectively; $\boldsymbol{q} \in \mathbb{R}^n$ is the displacement vector; $\boldsymbol{F} \in \mathbb{R}^n$ is the force vector.

To decompose structural response with non-proportional damping, a strategy is to rewrite Eqn 1 in state space, so that the *n* number of second-order differential equations can be converted to 2*n* number of first-order differential equations.

$$\boldsymbol{A}\dot{\boldsymbol{x}}(t) + \boldsymbol{B}\boldsymbol{x}(t) = \boldsymbol{P}(t) \tag{2}$$

where $\boldsymbol{x} \in \mathbb{R}^{2n}$ is the state vector. In order to make Eqns 1 and 2 equivalent, $\boldsymbol{x}$, $\boldsymbol{A}$, $\boldsymbol{B}$, $\boldsymbol{P}$ are defined as follows,

$$\boldsymbol{x}(t) = \begin{Bmatrix} \boldsymbol{q}(t) \\ \dot{\boldsymbol{q}}(t) \end{Bmatrix}_{2n\times 1} \tag{3}$$

$$\boldsymbol{A} = \begin{bmatrix} \boldsymbol{C} & \boldsymbol{M} \\ \boldsymbol{M} & \boldsymbol{0} \end{bmatrix}_{2n\times 2n}, \boldsymbol{B} = \begin{bmatrix} \boldsymbol{K} & \boldsymbol{0} \\ \boldsymbol{0} & -\boldsymbol{M} \end{bmatrix}_{2n\times 2n}, \boldsymbol{P}(t) = \begin{bmatrix} \boldsymbol{F}(t) \\ \boldsymbol{0} \end{bmatrix}_{2n\times 1} \tag{4}$$

Complex eigenvalues $s_i \in \mathbb{C}$ and eigenvectors $\boldsymbol{\psi}_i \in \mathbb{C}^{2n}$ $(i = 1,2,\dots,2n)$ can be obtained by solving the generalized eigenvalue problem of the state-space system,

$$(s_i\boldsymbol{A} + \boldsymbol{B})\boldsymbol{\psi}_i = \boldsymbol{0}, \qquad i = 1,2,\dots,2n \tag{5}$$

where $\boldsymbol{\psi}_i$ $(i = 1,2,\dots,2n)$ are the eigenvectors normalized with respect to $\boldsymbol{A}$ matrix, i.e., $\boldsymbol{\Psi}^{\mathrm{T}}\boldsymbol{A}\boldsymbol{\Psi} = \boldsymbol{I}_{2n\times 2n}$ with the eigenvector matrix defined as $\boldsymbol{\Psi} = [\boldsymbol{\psi}_1 \quad \boldsymbol{\psi}_2 \quad \dots \quad \boldsymbol{\psi}_{2n}] \in \mathbb{C}^{2n\times 2n}$. The superscript 'T' represents matrix transpose. As a result, denoting the diagonal eigenvalue matrix $\boldsymbol{S} =$

$\mathrm{diag}(s_1, s_2, \dots, s_{2n}) \in \mathbb{C}^{2n\times 2n}$, we have $\boldsymbol{\Psi}^{\mathrm{T}}\boldsymbol{B}\boldsymbol{\Psi} = -\boldsymbol{S}$. It is also well known that the complex-valued eigenvector $\boldsymbol{\psi}_i$ can be expressed as

$$\boldsymbol{\psi}_i = \begin{Bmatrix} \boldsymbol{\phi_i} \\ s_i\boldsymbol{\phi_i} \end{Bmatrix} \tag{6}$$

where $\boldsymbol{\phi_i}$ is an $n \times 1$ complex vector, which represents the modal displacements. Defining $\boldsymbol{z}(t) \in \mathbb{C}^n$ as the modal coordinate vector, the relationship between the state vector and modal coordinate vector is shown below,

$$\boldsymbol{x}(t) = \boldsymbol{\Psi}\boldsymbol{z}(t) \tag{7}$$

Substituting Eqn 7 into Eqn 2, we get

$$\boldsymbol{A}\boldsymbol{\Psi}\dot{\boldsymbol{z}}(t) + \boldsymbol{B}\boldsymbol{\Psi}\boldsymbol{z}(t) = \boldsymbol{P}(t) \tag{8}$$

Pre-multiplying Eqn 8 by $\boldsymbol{\Psi}^{\mathrm{T}}$ results in

$$\dot{\boldsymbol{z}}(t) - \boldsymbol{S}\boldsymbol{z}(t) = \boldsymbol{\Psi}^{\mathrm{T}}\boldsymbol{P}(t) \tag{9}$$

Because $\boldsymbol{S}$ is a diagonal matrix, Eqn 9 in vector form can be easily decoupled into $2n$ number of scalar differential equations. Recalling $\boldsymbol{\psi}_i = \begin{Bmatrix} \boldsymbol{\phi_i} \\ s_i\boldsymbol{\phi_i} \end{Bmatrix}$ and $\boldsymbol{P}(t) = \begin{bmatrix} \boldsymbol{F}(t) \\ \boldsymbol{0} \end{bmatrix}$, we get

$$\dot{z}_i(t) - s_i z_i(t) = {\boldsymbol{\phi}_i}^{\mathrm{T}}\boldsymbol{F}(t),\ i = 1,2,\dots,2n \tag{10}$$

Furthermore, through Fourier transform, Eqn 10 can be expressed in frequency domain as,

$$\mathrm{j}\omega\hat{z}_i(\omega) - s_i\hat{z}_i(\omega) = {\boldsymbol{\phi}_i}^{\mathrm{T}}\widehat{\boldsymbol{F}}(\omega) \tag{11}$$

where $\mathrm{j} = \sqrt{-1}$ is the imaginary unit; ω represents frequency. Using $\mathcal{F}\{\cdot\}$ to represent Fourier transform, $\hat{z}_i = \mathcal{F}\{z_i\}$ is the i-th modal coordinate and $\widehat{\boldsymbol{F}} = \mathcal{F}\{\boldsymbol{F}\}$ is the force vector in frequency domain.

Then, collect the terms in Eqn 11 and express the modal coordinate as

$$\hat{z}_i(\omega) = \frac{{\boldsymbol{\phi}_i}^{\mathrm{T}}\widehat{\boldsymbol{F}}(\omega)}{\mathrm{j}\omega - s_i} \tag{12}$$

In order to find the relationship between the input force and output displacement, we transform Eqn 7 into frequency domain and then substitute Eqn 12 into it,

$$\hat{\boldsymbol{x}}(\omega) = \boldsymbol{\Psi}\hat{\boldsymbol{z}}(\omega) = \sum_{i=1}^{2n} \boldsymbol{\psi}_i \hat{z}_i(\omega) = \sum_{i=1}^{2n} \frac{\boldsymbol{\psi}_i {\boldsymbol{\phi}_i}^{\mathrm{T}} \hat{\boldsymbol{F}}(\omega)}{\mathrm{j}\omega - s_i} \tag{13}$$

As shown in Eqn 3, the upper half of the state vector corresponds to displacement. So the frequency domain displacement $\hat{\boldsymbol{q}}$ can be expressed as below,

$$\hat{\boldsymbol{q}}(\omega) = \sum_{i=1}^{2n} \frac{\boldsymbol{\phi}_i {\boldsymbol{\phi}_i}^{\mathrm{T}} \hat{\boldsymbol{F}}(\omega)}{\mathrm{j}\omega - s_i} = \boldsymbol{H}(\omega)\hat{\boldsymbol{F}}(\omega) \tag{14}$$

Base on the derivation, $\boldsymbol{H} = \sum_{i=1}^{2n} \frac{\boldsymbol{\phi}_i {\boldsymbol{\phi}_i}^{\mathrm{T}}}{\mathrm{j}\omega - s_i} \in \mathbb{C}^{n \times n}$ is the receptance (displacement) FRF matrix, which represents the mapping from force input to displacement output.

Eqn 15 shows the (r, e) entry in the receptance matrix, which represents the input-output relationship from excitation at the *e*-th DOF to the response at the *r*-th DOF.

$$H_{r,e}(\omega) = \sum_{i=1}^{2n} \frac{\phi_{r,i}\phi_{e,i}}{\mathrm{j}\omega - s_i} \tag{15}$$

where $\phi_{r,i}$ and $\phi_{e,i}$ are the *r*-th and *e*-th entry of the *i*-th complex modal displacement vector $\boldsymbol{\phi}_i$, respectively.

To derive the FRFs from ground excitation to structural response, a similar approach is adopted as used by Hong *et al*. (2016). For an *n*-DOF shear-frame structure, the displacement at DOF-*r* caused by ground acceleration (A_{g}) is calculated as the summation of all contributions to displacement at DOF-*r* caused by the equivalent earthquake forces at all DOFs. Therefore, the analytical form of the FRFs with ground excitation can be extended from Eqn 15. Let $X_{r,e}(\omega)$ represent displacements at DOF-*r* due to $F_e(\omega)$, the excitation at DOF-*e* in frequency domain; and m_e be the lumped mass at DOF-*e*.

$$X_{r,\mathrm{g}}(\omega) = \sum_{e=1}^{n} X_{r,e}(\omega) = \sum_{e=1}^{n} H_{r,e}(\omega)F_e(\omega) = \sum_{e=1}^{n} -H_{r,e}(\omega)A_{\mathrm{g}}(\omega)\, m_e \tag{16}$$

The receptance for response at location *r* due to ground excitation can be derived from Eqn 16 :

$$H_{r,\mathrm{g}}(\omega) = \frac{X_{r,\mathrm{g}}(\omega)}{A_{\mathrm{g}}(\omega)} = \sum_{e=1}^{n} -H_{r,e}(\omega)\, m_e = \sum_{i=1}^{2n} \frac{-\phi_{r,i} \sum_{e=1}^{n} m_e\, \phi_{e,i}}{\mathrm{j}\omega - s_i} \tag{17}$$

For other types of measurement data besides displacement, FRF formulation for ground excitation can be easily changed to other forms. These include the mobility, $Y_{r,\mathrm{g}}(\omega)$, which represents the velocity response, and accelerance, $A_{r,\mathrm{g}}(\omega)$, which represents the acceleration response.

$$Y_{r,\mathrm{g}}(\omega) = \mathrm{j}\omega H_{r,\mathrm{g}}(\omega) \tag{18}$$

$$A_{r,\mathrm{g}}(\omega) = -\omega^2 H_{r,\mathrm{g}}(\omega) \tag{19}$$

2.2 Calculation of frequency response function from experimental data

In a large number of literatures related to FE model updating through FRFs, researchers only devoted their efforts in analytical FRF formulation rather than on how to calculate the experimental FRF through test data. It is well know that if the signal is polluted by noise, the model updating results are easy affected. However, measurement noise is impossible to avoid in experimental testing, which calls for the need of advanced FRF estimators to calculate the experimental FRFs. Researchers can choose different estimators to calculate the experimental FRF depending on their needs. For convenience, H_1 estimator (Schoukens and Pintelon 1990), as one of the most commonly used, is adopted here.

$$H_1(\omega) = \frac{S_{xy}(\omega)}{S_{xx}(\omega)} \tag{20}$$

where S_{xy} is the cross-spectral density between the excitation force and response signal; S_{xx} is the auto-spectral density of the response signal.

3 Frequency response function-based model updating approach and optimization procedures

3.1 Analytical vector form of frequency response functions for model updating

Because of the damping effect, the FRF formulations in Eqns 17 to 19 are complex-valued. Experiences suggest that the use of FRF magnitude (i.e. $\overline{H}_{r,\mathrm{g}}(\omega)$, $\bar{A}_{r,\mathrm{g}}(\omega)$) provide better results than the use of either the real part or the imaginary part of FRF or their combinations in the model updating process.

$$\bar{H}_{r,\mathrm{g}}(\omega) = \left|H_{r,\mathrm{g}}(\omega)\right| \tag{21}$$

The expression in Eqn 21 is a scalar representing magnitude evaluated at frequency ω. To include FRF values at multiple frequency points of interest, as well as FRFs from multiple response DOFs, a long vector is formulated as below,

$$\boldsymbol{H}^{\mathrm{Ana}} = \left\{ \left[\bar{H}_{r_a,\mathrm{g}}(\omega_1), \cdots, \bar{H}_{r_a,\mathrm{g}}\left(\omega_{n_\omega}\right)\right], \cdots, \left[\bar{H}_{r_p,\mathrm{g}}(\omega_1), \cdots, \bar{H}_{r_p,\mathrm{g}}\left(\omega_{n_\omega}\right)\right]\right\}^{\mathrm{T}} \tag{22}$$

The subscripts r_a, …, r_p represent different response DOFs. ω_i (i =1,…, n_ω) is an interested frequency point, an n_ω is the total number of interested frequency points.

The main objective of the model updating is to minimize the difference between analytical and experimental FRFs. $\boldsymbol{H}^{\mathrm{Ana}}$ is the long analytical FRF vector, and $\boldsymbol{H}^{\mathrm{Exp}}$ is the experimental counterpart. Both $\boldsymbol{H}^{\mathrm{Exp}}$ and $\boldsymbol{H}^{\mathrm{Ana}}$ should be written in the same sequence as show in Eqn 22.

3.2 Frequency response function-based model updating

For a linear structure, the stiffness and mass matrices can be expressed as matrix functions of the updating variables $\boldsymbol{\alpha} \in \mathbb{R}^{n_\alpha}$ and $\in \mathbb{R}^{n_\beta}$, respectively. Notation n_α and n_β represent the total number of updating variables associated with stiffness and mass, respectively; the r-th entry of $\boldsymbol{\alpha}$ and $\boldsymbol{\beta}$, α_r and β_r are the relative change percentage associated with physical parameters to be updated, such as Young's modulus, support spring stiffness and mass density, etc.

$$\boldsymbol{K} = \boldsymbol{K}_0 + \sum_{r=1}^{n_\alpha} \alpha_r \boldsymbol{K}_{0,r} \tag{23}$$

$$\boldsymbol{M} = \boldsymbol{M}_0 + \sum_{r=1}^{n_\beta} \beta_r \boldsymbol{M}_{0,r} \tag{24}$$

where $\boldsymbol{K}_0$ and $\boldsymbol{M}_0$ are the constant nominal stiffness and mass matrices, respectively, as the starting point of the modeling; $\boldsymbol{K}_{0,r}$ and $\boldsymbol{M}_{0,r}$ are the constant influence matrices which corresponding to α_r and β_r, respectively.

In this research, general viscous damping is assumed for simulating more practical structural system. As mentioned by Chopra (2001), it is impractical to build the damping matrix in the form of building stiffness matrix. Therefore, every entry in the damping matrix can be defined as an optimization variable. In order to reduce the number of the damping updating variables, the damping matrix is constrained to be symmetric positive definite (denoted as $\boldsymbol{C} > 0$).

The complete optimization problem is provided as follows.

$$\text{minimize} \quad \left\| \boldsymbol{H}^{\text{Ana}}(\boldsymbol{\alpha}, \boldsymbol{\beta}, \boldsymbol{C}) - \boldsymbol{H}^{\text{Exp}} \right\|^2 \tag{25a}$$

$$\text{subject to} \quad (s_i \boldsymbol{A} + \boldsymbol{B})\boldsymbol{\psi}_i = \boldsymbol{0} \tag{25b}$$

$$\boldsymbol{H}^{\text{Ana}} = \left\{ \left[\overline{H}_{r_a,\text{g}}(\omega_1), \cdots, \overline{H}_{r_a,\text{g}}\left(\omega_{n_\omega}\right)\right], \cdots, \left[\overline{H}_{r_p,\text{g}}(\omega_1), \cdots, \overline{H}_{r_p,\text{g}}\left(\omega_{n_\omega}\right)\right] \right\}^{\text{T}} \tag{25c}$$

$$H_{r,\text{g}}(\omega) = \sum_{i=1}^{m} \frac{-\phi_{r,i} \sum_{e=1}^{n} m_e \, \phi_{e,i}}{\text{j}\omega - s_i} \tag{25d}$$

$$\boldsymbol{\alpha}^{\text{l}} \leq \boldsymbol{\alpha} \leq \boldsymbol{\alpha}^{\text{u}} \; ; \; \boldsymbol{\beta}^{\text{l}} \leq \boldsymbol{\beta} \leq \boldsymbol{\beta}^{\text{u}} \tag{25e}$$

$$\boldsymbol{C} > 0 \tag{25f}$$

where $\|\cdot\|$ can be any norm function; $\boldsymbol{\alpha}$, $\boldsymbol{\beta}$, $\boldsymbol{C}$ are the selected optimization variables. Lower bound (superscript l) and upper bound (superscript u) are set for those updating variables corresponding to physical parameters. m is the total number of analytical modes used in model updating.

3.3 Optimization procedures

The frequency response function-based model updating approach is formulated as a constrained optimization problem in Eqn 25. There are several optimization algorithms that can be utilized for finding the optimum value for the variables, such as nonlinear least-square, particle swarm and Newton method, etc. In this research, a constrained nonlinear multivariable function solver 'fmincon' in MATLAB optimization toolbox (Math Works Inc. 2015) is adopted for solving the problem. In general, the optimization problem in Eqn 25 is non-convex and there is no optimization algorithm can guarantee the global optimality of the solution. In order to increase the possibility of finding the global optimal value for the problem, 'Global Search' in MATLAB is recommended to use together with 'fmincon'.

3.3.1 'fmincon' in MATLAB

The solver ‘fmincon’ seeks a minimum of the objective function value to match the analytical FRFs with the experimental FRFs. One of the many advantages is that both equality and inequality constraints are allowed in this solver. In addition, the lower and upper bounds for optimization variables are allowed. Four algorithms are implemented in ‘fmincon’ optimization solver, including the trust region reflective algorithm, active set algorithm, sequential quadratic programming (SQP) algorithm and interior-point algorithm. Among them, the trust region reflective algorithm needs to provide gradient information of the objective function by the user. From this point of view, the algorithm is not suitable for those objective functions whose gradients are difficult to explicitly write in closed form. Other than this limitation, the trust region reflective algorithm allows user to set either bounds or linear equality constraints. Active set algorithm and SQP algorithm are not suitable for large scale problem. Since the interior-point algorithm does not have obvious drawbacks, it is adopted as the first trial. The interior-point algorithm is essentially a quasi-Newton method, which calculates the Hessian approximation by the BFGS algorithm. The interior-point algorithm will first attempt a direct-step to solve the KKT conditions; if unsuccessful, a conjugate-gradient search will be adopted instead. When numerically evaluating the gradient, based on the author’s experience, the minimum change of updating variables (‘DiffMinChange’ option) can be set comparatively larger for a highly nonlinear optimization problem. Allowing larger minimum change makes the gradient calculation more robust against inaccurate objective function evaluations due to numerical noises.

3.3.2 ‘Global Search’ in MATLAB

Because of the non-convexity of the objective function, the ‘fmincon’ solver may easily get trapped into a local minimum or even stop near the initial starting point. In order to increase the chance to find a more optimal solution for the objective function, the optimization procedure can be started from many initial points. ‘Global Search’ in MATLAB as a global optimization toolbox can help generate many initial points for local solvers using a scatter-search algorithm. It analyzes the initial points and only accept those points who can improve the optimization results. The drawback of ‘Global Search’ in MATALB is that it can only run together with local solver ‘fmincon’. The number of starting points can be set by experience. The more starting points one uses, the higher the chance is in finding a better solution with a smaller objective function value. On the other hand, more starting points usually consume more computing time.

4 Experimental validation

In this section, the performance of the FRF-based model updating approach is validated through a four-story shear-frame laboratory structure. How to select the frequency points for matching the FRFs is also discussed.

4.1 Shake table (ground excitation) test

The test structure shown in Figure 1 is mounted on a small shake table. All the column bars and floor plates are made of the same aluminum material. Every floor plate has the same mass 4.64kg. As initial starting point for mass variables, this number does not include the mass of sensor instrumentation on each floor; the model updating is expected to update the total mass so that equivalently the instrumentation mass is identified through updating. Every story has 8 thin column bars riveted to the plate. The rectangular section is 0.0254m × 0.00159m. The Young's modulus of the material is 63GPa. The total height of the structure is 1.182m (0.305m×3 + 0.267m). Fixed connections are applied at the bottom of the every column. This structure can be idealized as a 4-DOF system since every floor can be taken as a rigid mass, and the lateral stiffness are mainly provided by bending of the columns. The model updating is expected to identify the inter-story shear stiffness provided by the columns. There are in total 5 accelerometers and 5 linear variable differential transformers (LVDT) installed on the structure for measuring the vibration. The accelerometer and LVDT on the same floor are interfaced with one wireless sensing system, *Martlet* (Kane *et al*. 2014). More detailed descriptions of the structure and sensors can be found in Hong *et al*. (2016).

During the shake table test, the ground earthquake is simulated by a chirp excitation which changes from 0Hz to 10Hz within 60s. The sampling frequency of the *Martlet* is set to be 200Hz. Figure 2 shows the measured ground excitation time history. To get enough FRF data for model updating, the experimental accelerances and receptances are calculated using the measured acceleration and displacement response on every floor with the ground excitation, respectively. Figure 3 shows acceleration and displacement responses of the 4th floor.

4.2 Frequency points selection

Figure 4 and figure 5 show the overlay plots of accelerances and receptances in frequency domain, respectively. In order to illustrate the resonance areas more clearly, all FRFs are plotted in dB form. There are 4 obvious peaks which correspond to 4 resonant frequencies. Although a large number of FRF points can be obtained from these curves, it is not recommended to use all frequency points for model updating. First, we notice the regions away from resonances are not as clean as the resonant areas, because the influence of sensor noise is more predominant at the regions with low energy near anti-resonances. FRF data in such regions with low signal-to-noise ratio (SNR) negatively affect the model updating accuracy, and thus, should not be used for matching with the analytical FRFs towards model updating. Since damping parameters in this structure are important optimization variables and damping effect mainly manifests around the resonances, the peak areas of each FRF curve are chosen as the target for matching the analytical FRFs. From our experience, half-power bandwidth method is recommended to identify the target frequency points around each resonance. Esfandiari *et al*. (2016) mentioned the importance of using FRF data in high frequency range for model updating, because high frequency corresponds to local structural vibration patterns. Therefore, it would be better to include the 4th peak (although they have relatively low amplitude) for model updating. In this study, the FRF calculated from responses on all floors will be used for a updating, although the updating can still be performed using data from only some floors.

4.3 Model updating result

For this 4-story structure, the optimization variables include the inter-story shear stiffness of each floor, the mass of each floor, and each entry of the damping matrix. Mainly contributed by shear stiffness from the fixed-end columns, the initial story stiffness values are calculated based on the nominal Young’s modulus of the material and the fix-end assumptions. The initial mass value is the 4.64 kg plate mass. The reason to choose the mass of each floor as updating variables is that the mass of sensor instrumentation cannot be neglected on this laboratory-scale structure. It is easy to find that mass and stiffness information cannot be all updated through most modal property-based updating approaches, because of the scaling effect to stiffness and mass in the eigenvalue equation. Unlike these modal property-based updating approaches, the use of eigenvectors normalized with respect to $\boldsymbol{A}$ matrix (Eqn 5) prevents the scaling effect, allowing us to update all mass and stiffness values simultaneously. The lower bounds and upper bounds for mass and stiffness allow the variables to change in a reasonable range.

Table 1 summarizes the model updating results for the variables related to mass and stiffness. Analytical receptances and accelerances are updated through Eqn 25, respectively. In the last row of Table 1, the average updated values of mass and stiffness variables are calculated. Since damping updating is most difficult, we set the initial starting damping matrix as a Rayleigh damping matrix. The Rayleigh damping coefficients are chosen based on experience. In addition, during the updating process, the lower bounds and upper bounds for damping updating variables are set to be relatively large.

Figure 6 shows an example of the updating FRF plots using the proposed model updating approach. Figure 6(a) compares the initial, the experimental and updated accelerance $\boldsymbol{A}_{3,\mathrm{g}}$. Figure 6(b) shows the comparison for receptance $\boldsymbol{H}_{3,\mathrm{g}}$. The comparison plots demonstrate that the proposed approach is able to well match analytical FRFs with experimental ones. In particular, the peak areas for these updated FRF curves can match well with the peak areas of experimental FRF curves. Because damping controls the amplitude of the FRF at frequency points close to resonances, this result shows damping of the structure is updated with good accuracy. The frequency domain assurance criterion (FDAC) (Pascual *et al*. 1997) value can be utilized to compare the similarity of the peak areas between the updated and experimental FRFs. A value 1 means perfect correlation, 0 means no correlation at all. The FDAC value in Figure 6(a) is 0.987 and the FDAC value in Figure 6(b) is 0.991.

In order to further verify the model updating results, a time domain comparison is also conducted. The average value of each optimization variable is used for building a new analytical model; the measured ground acceleration is fed into the model for simulating dynamic responses. Figure 7(a) shows an overall comparison between the simulated acceleration (from the new model) and the experimental acceleration on the 4$^{\text{th}}$ floor. Figure 7(b) is a close-up comparison for a three-second duration with the highest amplitude, demonstrating a close match between simulated and experimental time histories. In addition, Figure 8(a) shows the overall comparison between the simulated displacement from the new model and the experimental displacement on the same floor. Figure 8(b) also gives a close-up comparison. All figures illustrate excellent agreement between the simulated results and the experimental data, which demonstrates the ability of the proposed FRF-based model updating approach in obtaining an accurate FE model to represent the structure.

4.4 Performance of the optimization toolbox

As discussed in section 3.3, 'fmincon' and 'Global Search' in MATLAB toolbox are shown to be suitable for solving the optimization problem in this study. One of the biggest advantages is the simplicity for implementation. For this research, the convergence limits for objective function value and each optimization variable are set as 10^{-6} and 10^{-8}, respectively. In order to achieve more optimal updating results, a comparatively large number (10,000) of trial starting points are adopted for 'Global Search'. Although more trial points mean higher time consumption, the inherent scatter search algorithm automatically eliminates the less promising starting points, effectively reducing the computation. The results shown in section 4.3 indicate good performance of the optimization toolbox for updating the 4-story structure. However, for more complex structures, the non-convexity of the objective function may be more significant, thus the optimization difficulty can increase accordingly.

5 Summary and future work

A summary of this work is first provided as follows:

1) The proposed FRF-based model updating approach has been investigated through a laboratory structure. In order to consider general viscous damping, the analytical formulation of FRF was derived in state space. Unlike other FRF-based model updating approaches, the proposed approach does not require the analytical FRF sensitivity matrix (which is impossible or difficult to get in most cases) for each updating variable. No model reduction or modal expansion is needed.

2) The proposed model updating approach can be easily implemented using state-of-the-art optimization toolboxes. MATLAB optimization solvers 'fmincon' and 'Global Search' have been

carefully discussed. Leveraging these optimization techniques, it is more likely to find an objective function value closer to the global minimal for the non-convex problem.

3) The proposed approach was successfully applied on the model updating of a 4-story structure. Two different types of measured FRFs (accelerance and receptance) from a shake table test are used in the updating process. The criterion for choosing appropriate frequency ranges has been discussed through this study. The results show that the FRFs of the updated model very closely match with the experimentally measured FRFs of the actual structure. Furthermore, a time-domain comparison between the simulated response and experimental response was conducted to verify the effectiveness of the model updating.

In the future, the FRF-based FE model updating will be performed on an actual space frame bridge, using field measurement data. More optimization algorithms will be studied for achieving better updating result.

Acknowledgement

This research is partially supported by the National Natural Science Foundation of China (51508474) and the China Scholarship Council. The third author acknowledges the support from U.S. National Science Foundation (CMMI-1150700). The authors also wish to express their gratitude to Xinjun Dong and Xi Liu in Georgia Institute of Technology for their assistance. Any opinions, findings, and conclusions or recommendations expressed in this publication belong to those authors and do not necessarily reflect the view of the sponsors.

References

Antoni J., Wagstaff P., Henrio J. C. (2004) “Hα-a consistent estimator for frequency response functions with input and output noise”, IEEE transactions on instrumentation and measurement, Vol. 53, No. 2, pp. 457–465.

Asma F., Bouazzouni A. (2005). “Finite element model updating using FRF measurements”, Shock and

Vibration, Vol. 12, No. 5, pp. 377–388.

Avitabile P., O'callahan J. (2001). “Dynamic expansion of frequency response functions for the full FRF matrix”, Proceedings of SPIE: the International Society for Optical Engineering, pp. 887–896.

Brito, V. L., Pena, A. N., Pimentel, R. L., and de Brito, J. L. V. (2014). “Modal Tests and Model Updating for Vibration Analysis of Temporary Grandstand”, Advances in Structural Engineering, vol. 17, No. 5, pp. 721–734.

Chopra A. K. (2001). Dynamics of structures: theory and applications to earthquake engineering, Prentice Hall Pubishers, Upper Saddle River.

Esfandiari A., Rahai A., Sanayei M., Bakhtiari-nejad, F. (2016). “Model updating of a concrete beam with extensive distributed damage using experimental frequency response function”, Journal of Bridge Engineering, Vol. 21, No. 4, pp. 04015081.

Friswell, M. I. and Mottershead, J. E. 1995. Finite element model updating in structural dynamics, Kluwer Academic Publishers, Dordrecht & Boston.

Hernandez, E. M. and Bernal, D. (2013). “Iterative finite element model updating in the time domain”, Mechanical Systems and Signal Processing, vol. 34, No. 1, pp. 39–46.

Hong Y., Liu X., Dong X., Wang Y., Pu Q. (2016). “Experimental model updating using frequency response functions”, Proceedings of SPIE: Sensors and Smart Structures Technologies for Civil, Mechanical, and Aerospace Systems, J.P. Lynch, ed., Las Vegas, March, 2016, pp. 980325.

Imregun, M. and Visser, W. J. (1991). “A review of model updating techniques”, The Shock and Vibration Digest, Vol. 23, No.1, pp. 9–20.

Imregun M., Sanliturk K. Y., Ewins D. J. (1995). “Finite element model updating using frequency response function data: II. Case study on a medium-size finite element model”, Mechanical Systems and Signal Processing, Vol.9, No.2, pp. 203–213.

Jaishi B. and Ren W. X. (2005). “Structural finite element model updating using ambient vibration test results”, Journal of Structural Engineering, Vol. 131, No. 4, pp. 617–628.

Kane M., Zhu D., Hirose M., Dong X., Winter B., Häckell M., Lynch J. P., Wang Y. and Swartz A. (2014). “Development of an extensible dual-core wireless sensing node for cyber-physical systems”, SPIE Smart Structures and Materials+ Nondestructive Evaluation and Health Monitoring, San Diego, April, pp. 90611U-90611U-19.

Lin R. M. and Ewins D. J. (1994). “Analytical model improvement using frequency response functions”, Mechanical Systems and Signal Processing, Vol.8, No.4, pp. 437–458.

Lin R. M. and Zhu J. (2009). “On the relationship between viscous and hysteretic damping models and the importance of correct interpretation for system identification”, Journal of Sound and Vibration, Vol.325, No. 1, pp. 14–33.

Lu Y., Tu Z. (2004). “A two-level neural network approach for dynamic FE model updating including damping”, Journal of Sound and Vibration, Vol.275, No. 3, pp. 931–952.

MathWorks Inc. (2015). Optimization ToolboxTM User's Guide, R2015b ed. Natick, MA.

Pascual, R., Golinval J. C., Razeto M. (1997). “A frequency domain correlation technique for model correlation and updating”, Proceedings of SPIE: The International Society for Optical Engineering, February, pp. 587-592.

Pradhan S. and Modak S. V. (2012). “Normal response function method for mass and stiffness matrix updating using complex FRFs”, Mechanical Systems and Signal Processing, Vol.32, pp. 232–250.

Schoukens J., Pintelon R. (1990). “Measurement of frequency response functions in noisy environments”, IEEE Transactions on Instrumentation and Measurement, Vol. 39, No. 6, pp. 905–909.

Sipple J. D. and Sanayei M. (2014). “Finite element model updating using frequency response functions and numerical sensitivities”, Structural Health Monitoring, Vol. 21, No. 5, pp. 784–802.

Tshilidzi M. and Sibusiso S. (2005). “Finite element model updating using bayesian framework and modal properties”, Journal of Aircraft, Vol. 42, No. 1, pp. 275–278.

Yang, J. N., Huang H. W., Pan S. W. (2009) “Adaptive quadratic sum-squares error for structural damage identification”, Journal of Engineering Mechanics-ASCE, vol.135, No.2, pp. 67–77.

Zhu, D., Dong, X. and Wang Y. (2016) “Substructure Stiffness and Mass Updating through Minimization of Modal Dynamic Residuals”, Journal of Engineering Mechanics, vol. 142, No.5, pp. 04016013.

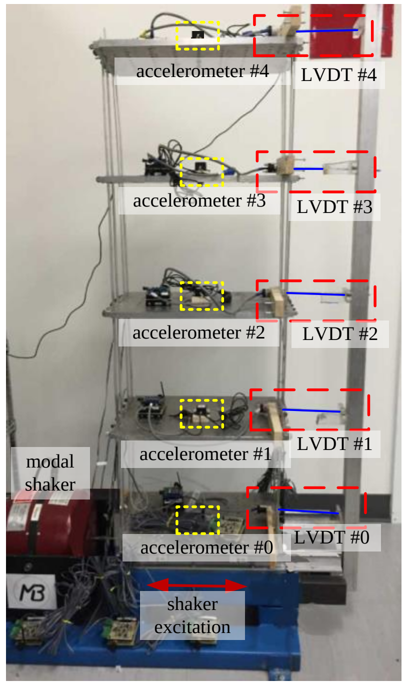

Figure 1. Frame structure with experimental setup

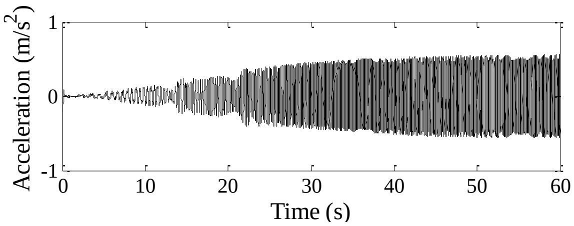

Figure 2. Ground excitation time history

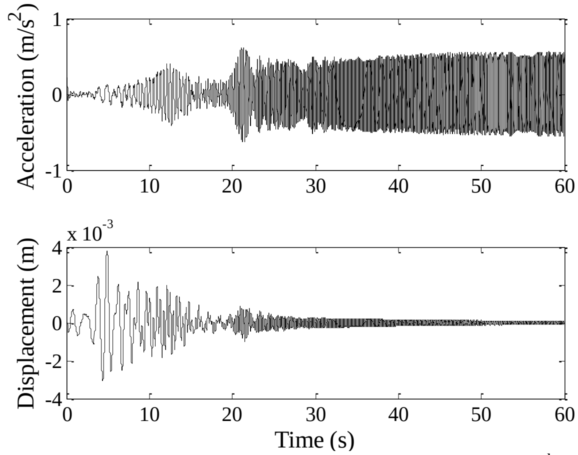

Figure 3. Acceleration and displacement responses of the 4th floor

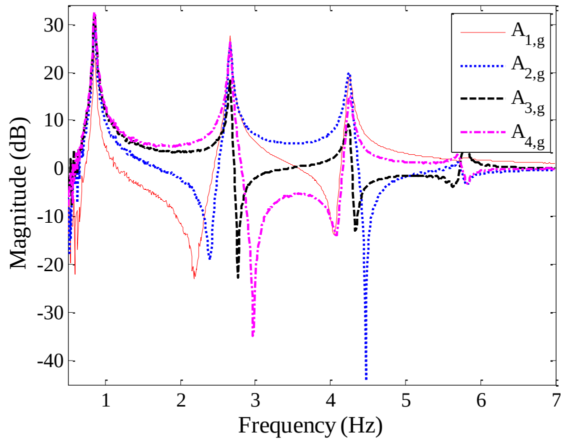

Figure 4. Overlay of accelerance plots for all floors

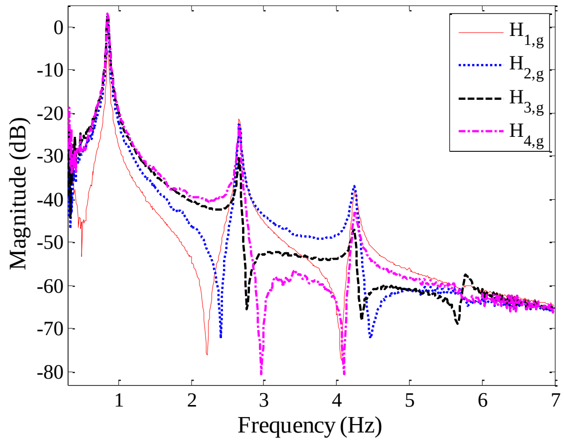

Figure 5. Overlay of receptance plots for all floors

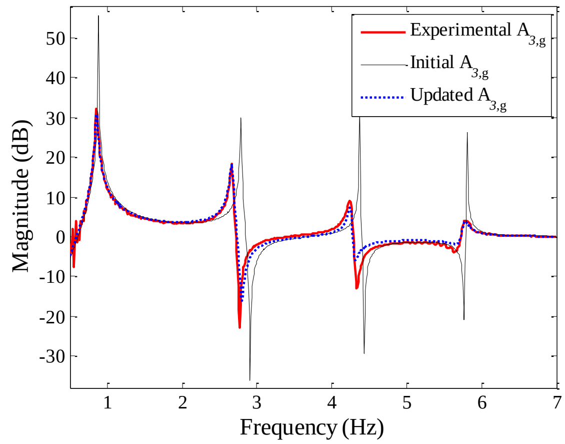

(a) Accelerance $\boldsymbol{A}_{3,\mathrm{g}}$

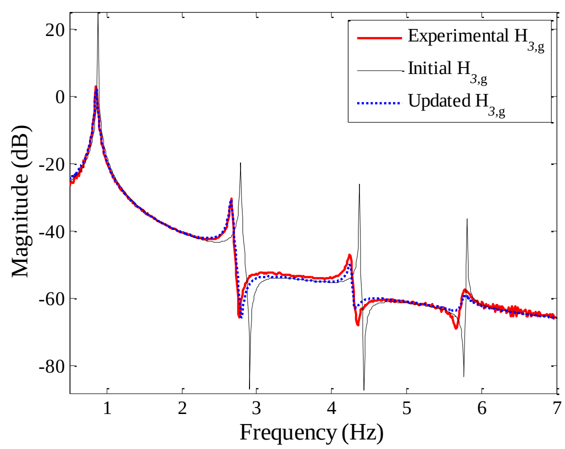

(b) Receptance $\boldsymbol{H}_{3,\mathrm{g}}$

Figure 6. Comparison of the initial, the experimental and the updated FRFs

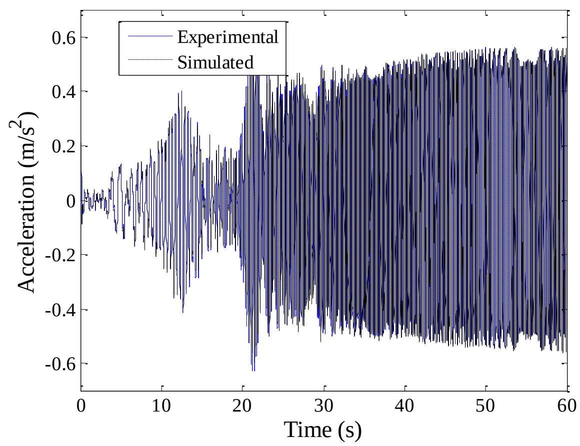

(a) Acceleration comparison on 4th floor

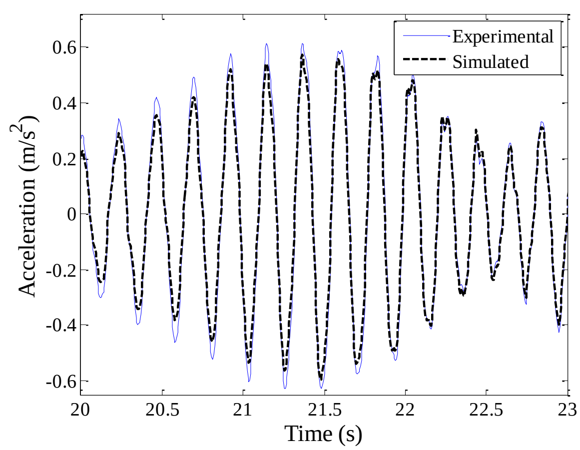

(b) Close-up acceleration comparison on 4th floor

Figure 7. Comparison between the experimental and simulated acceleration

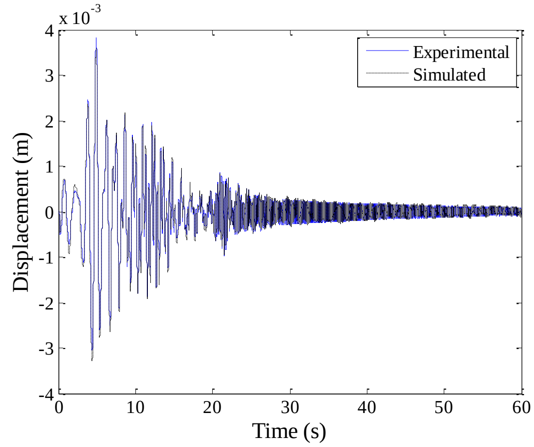

(a) Displacement comparison on 4th floor

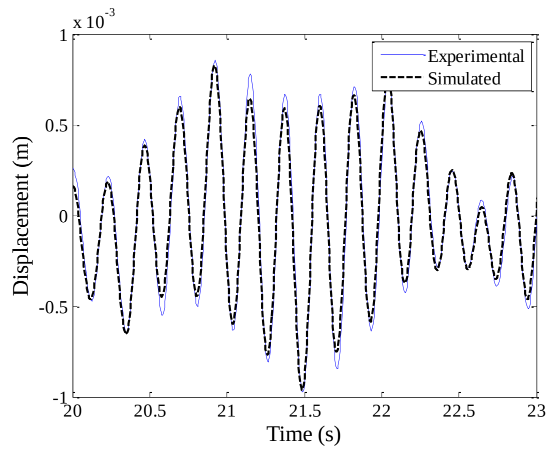

(b) Close-up displacement comparison on 4th floor

Figure 8 Comparison between the experimental and simulated displacement

Table 1 Model updating results from shake table test.

Parameter (kg or N/m)	m_1	m_2	m_3	m_4	k_1	k_2	k_3	k_4
Initial	4.64	4.64	4.64	4.64	1019	1217	1420	2473
Updated (Accelerance)	5.16	5.14	4.94	5.14	1049.71	1282.53	1385.56	2732.56
Updated (Receptance)	5.16	5.16	4.94	5.14	1060.25	1285.84	1368.70	2743.77
Average of the updated	5.16	5.15	4.94	5.14	1054.98	1284.19	1377.13	2738.17